2014-01-01

Diagnostics of an O2–He RF Atmospheric Plasma Discharge by Spectral Emission

Vladimir Milosavljevic
Technological University Dublin, vladimir.milosavljevic@tudublin.ie

Mick Donegan
University College Dublin

Patrick Cullen
Technological University Dublin, pj.cullen@tudublin.ie

See next page for additional authors

Recommended Citation

Milosavljevic, V., Donegan, M., Cullen, P.J. and Dowling, D.P. Diagnostics of an O2–He RF Atmospheric Plasma Discharge by Spectral Emission. Journal of the Physical Society of Japan 83, 014501 (2014). doi.org/10.7566/JPSJ.83

Funder: the Department of Agriculture, Food and the Marine, Ireland

Journal of the Physical Society of Japan 83, xxxxxx (2014)
http://dx.doi.org/10.7566/JPSJ.83.xxxxxx

Diagnostics of an O_2–He RF Atmospheric Plasma Discharge by Spectral Emission

Vladimir Milosavljević[1,2,3,4*], Mick Donegan[5], Patrick J. Cullen[1], and Denis P. Dowling[5]

[1]*BioPlasma Research group, Dublin Institute of Technology, Sackville Place, Dublin 1, Ireland*
[2]*Biosystems Engineering, University College, Dublin, Dublin 4, Ireland*
[3]*NCPST, Dublin City University, Dublin, Ireland*
[4]*Faculty of Physics, University of Belgrade, P.O.B. 368, Belgrade, Serbia*
[5]*School of Mechanical and Materials Engineering, University College Dublin, Belfield, Dublin 4, Ireland*

(Received March 12, 2013; accepted October 25, 2013; published online xxxx yy, zzzz)

In this paper optical emission spectroscopy (OES) is used as a Diagnostic technique for the measurement of atomic and molecular spectral emissions generated using a helium rf industrial atmospheric plasma jet system. The OES of neutral atomic spectral lines and molecular bands are investigated over a range of plasma process parameters. Wavelength resolve optical emission profiles suggest that the emission of helium's spectral lines shows that the high energy electrons have a larger influence than helium metastables on the overall spectral emission. Furthermore, the experimental data indicates that the use of high helium flow rates, in any confined open air plasma discharge, limits the significance of air impurities, e.g., nitrogen, for the creation and sustainability of plasma discharges in helium–oxygen gas chemistry.

1. Introduction

Atmospheric pressure, non-thermal helium plasma jets are increasingly used in many processing applications, due to their combination of inherent plasma stability and excellent reaction chemistry, which is often enhanced downstream of the plasma source. The majority of the atmospheric pressure plasmas are non-equilibrium at ambient temperature and are generated by electrical discharge. Despite their widespread usage, it remains largely unknown whether cold atmospheric plasma jets maintain similar characteristics, such as gas temperatures and particle flux, when they breakdown while arcing or whether they possess different operating modes.

Therefore, in order to ensure process reproducibility, the monitoring and control of plasma processes is essential in both laboratory and industrial environments. Most plasma systems, other than specialised laboratory plasma systems, do not facilitate intrusive plasma diagnostics (i.e., for collecting local plasma properties) or have plasma chambers with only one or two access points. It is also important to underline, that due to the high industrial demand for plasma technologies and the resulting competition between system manufacturers, many of these manufacturers come to the market with closed box plasma systems (typically a plasma generator and its matching network in the single box), which cannot be opened due to warranty issues. This leads to the situation where the only plasma diagnostic techniques available are optical techniques. Under these circumstances it is very challenging to develop an experimental approach, which would give a fundamental explanation of the impact of plasma physics on atomic physics, e.g., the role of metastable atoms, resonance energy levels, triplet and singlet energy scale, life time of electrons in an excited atom/molecular state, etc. One non-intrusive technique that has been successfully used for plasma diagnostics is optical emission spectroscopy (OES). A disadvantage of the OES technique is that the integration of measured signals must be carried out over a line of sight observation. Despite this limitation however, OES is commonly used to detect light emitted by excited species from plasma discharges.

The type of operating gas influences the stability of atmospheric plasma discharges. Helium gives rise to a stable homogeneous discharge, whereas nitrogen, oxygen and argon easily cause the transition into a filamentary discharge.[1)] Atmospheric plasma, propagating in the surrounding ambient air, can incur impurities due to the surrounding ambient atmosphere, which also follows the feed gas channel. The most dominant species in the atmosphere is nitrogen.[2)] In the vast majority of atmospheric plasma discharges, nitrogen dominates the ionic composition of atmospheric discharge and has an impact on the breakdown voltage. When nitrogen is added/mixed with helium plasma discharges, the helium emission lines are significantly quenched and the resulting plasma changes from a reddish colour to strong green. In the 300–450 nm spectral range, the strongest emission is the N_2^+ first negative system ($B^2\Sigma_u^+ \rightarrow X^2\Sigma_g^+$) and the N_2 second positive system ($C^3\Pi_u \rightarrow B^3\Pi_g$). On the other hand, nitrogen in most atmospheric plasma is not a carrier gas and therefore can dilute the plasma chemistry from the feed gas channel, acting as a contaminant gas. Moreover as nitrogen comes from the outside of the discharge channel and is always at ambient temperature, it effects the temperature of the plasma discharge.[3)] There is also an important role for nitrogen in the generation of NO_x (and other greenhouse gases), acid rain and other environmental problems. Therefore minimizing the influence of nitrogen, as an unwanted addition, to plasma discharges in the ambient air is an important challenge. This is especially true because the plasma chemical conversion of N_2 and O_2 into NO_x is a very efficient process.[4)]

Our main motivation in the present work is (1) to investigate the influence of high-energy electrons and helium metastables on the overall spectral emission, (2) to study how high helium flow rates, in a confined open air plasma discharge, limits the significance of air impurities in the creation and sustainability of plasma discharges in the helium–oxygen gas chemistry, (3) to minimize the influence of nitrogen, as an unwanted contaminant to plasma discharges in the ambient air, thus limiting the important role of nitrogen in the generation of greenhouse gases etc., (4) to explore the production channel of oxygen radicals by

direct electron impact (excitation process) from the ground state of the O I in the high helium flow rate plasma discharge.

2. Experimental

Included in this work is the use of OES for recording the absolute spectral emissions of the atomic and molecular lines associated with helium, oxygen, nitrogen and hydrogen. Analysis of these species spectral intensities will assist in the development of optimised plasma processing parameters for treatments such as polymer surface activation, the removal of contaminates etc.

2.1 Helium spectral emission

Helium has, as it is well known, two independent sets of energy levels (singlet and triplet), and an ionization limit of 24.59 eV.[5] There are triplet and singlet excited energy levels in a neutral helium atom (He I) and electron transition among these are forbidden in dipole–dipole approximations. In general, the intercombination of spontaneous transition probabilities from triplet to singlet for neutral helium is very low. Therefore both of the spectral emissions (from the triplet and singlet energy levels), should be taken into account separately for a valid representation of a full helium spectral radiation. The intensity of helium was monitored over six prominent atomic helium spectral lines. There are three spectral lines from the helium triplet spectra He388 (He I; $\lambda = 388.865$ nm; $2s^3S_1$–$3p^3P^o_{1,2}$), He587 (He I; $\lambda = 587.562$ nm; $2p^3P^o_{1,2}$–$3d^3D_{1,2,3}$) and He706 (He I; $\lambda = 706.519$ nm; $2p^3P^o_{1,2}$–$3s^3S_1$). There are also three spectral lines from the helium singlet spectra He501 (He I; $\lambda = 501.568$ nm; $2s^1S_0$–$3p^1P^o_1$), He667 (He I; $\lambda = 667.815$ nm; $2p^1P^o_1$–$3d^1D_2$) and He728 (He I; $\lambda = 728.135$ nm; $2p^1P^o_1$–$3s^1S_0$).[5] Helium's high metastable energy levels, which act as a "reservoir of energy", make it ideal for use for plasma processing.[1,6] Density of helium metasables atoms can be measured by laser absorption spectroscopy[7] and the results of these experiments are dependant on helium gas flow rate. The measurement of He metasable densities in Ref. 7 have been performed for two plasma systems, one of which (the mesh-type), is similar to the plasma jet in this work. The results presented for the mesh-type system[7] indicate that at atmospheric pressure helium metasable densities decrease with increasing gas flow rate. Moreover, Fig. 5 (in Ref. 7) indicates that helium higher flow rates quench the excited species, especially the long-lived metasable atoms, causing a decrease in the discharge current with increasing gas flow rates. On the helium triplet energy scale, there is a metastable energy level at $1s2s(^3S_1)$ with an energy of 19.82 eV. Using OES, this energy level can be observed as the He388 spectral line emission and therefore the spectral intensity of this atomic line can be used for the monitoring of a metastable helium atom in the triplet state. The $1s2s(^1S_0)$ is a metastable energy level in the helium singlet state with energy of 20.62 eV. The lower energy level of He501 is $2s(^1S_0)$. Therefore the spectral intensity of the He501 is proportional to the metastable density of helium singlet atoms. Four additional helium spectral lines, discussed in this work, all have lower energy levels, which are the same as the helium resonate levels. They are He587 and He706 lines which each have lower energy level $1s2p(^3P^o_1)$ with the energy of 20.96 eV, and this is the resonate level of the helium triplet state. The He667 and He728 have the lower energy level $1s2p(^1P^o_1)$ with a energy of 21.22 eV,[5] and this energy level is a resonant level of the helium singlet state. The lifetime of electrons in resonate energy levels are much shorter than the lifetime in an "ordinary" excited energy level[5] and is many orders of magnitude shorter than an electrons life time at metastable energy levels. Because of this the quenching of resonate energy levels is negligible and therefore an electron transition that ends on a resonate energy level may be use for the monitoring of an atom's density in its ground state.

2.2 Oxygen spectral emission

Oxygen species were studied in the He plasma using measurements of atomic (O I) and molecular (O_2) spectral emissions. All recorded atomic oxygen spectral lines are triplets.[5] The following atomic oxygen triplet spectral lines are recorded: O615 (O I; $\lambda = 615.598$, 615.677, and 615.818 nm; $3p^5P_{1,2,3}$–$4d^5D^o_{1,3,4}$), O777 (O I, $\lambda =$ 777.194, 777.417, and 777.539 nm; $3s^5S^o_2$–$3p^5P_{1,2,3}$) and O845 (O I, $\lambda = 844.625$, 844.636, and 844.676 nm; $3s^3S^o_1$–$3p^3P_{0,1,2}$). The O615 spectral emission comes from the high laying excited energy level of 12.75 eV.[5] The lower energy level of the O615 triplet coincides with the upper states of the O777 triplet, with an energy of 10.74 eV. Therefore the O615 triplets increase in intensity emission, would result in a change of the relative intensity of the individual lines of the 777 triplet, and this could lead to errors in using the spectral intensity of 777 triplet for plasma diagnostics, since the one of O777 spectral line is used for actinometry.[8] The third recorded atomic oxygen spectral line, O845, has the energy threshold of the excited states of 10.99 eV.[5] The O615, O777, and O845, are created by direct excitation from a ground state, but could be also created over a O_2 dissociation. The energy threshold for O_2 dissociation, and selected spectral lines, are: 16.1 eV (O777), 16.3 eV (O845), and 18.0 eV (O615). These energies are lower than the energy of helium metastables, therefore the dissociation of molecular oxygen must be taken into account in the interpretation of atomic oxygen spectral line intensity.

The neutral oxygen molecule does not readily show an emission spectrum, as the spectral emissions of molecular oxygen generally have very weak spectral emissions, however these can be observed under optimised atmospheric pressure conditions. The A-band (O_2760) is the only recorded molecular oxygen emission in this work. The A-band has a band-head emission at $\lambda = 759.37$ nm and belongs to a transition $b^1\Sigma_g^+$–$X^3\Sigma_g^-$.[9] Oxygen molecules have seven long-living metastable states located in the energy diagram below the first dissociation limit, at approximately 5.1 eV. The upper energy state ($b^1\Sigma_g^+$) of the O_2760 emission is one of molecular oxygen metastables with energies of 1.63 eV. Transition from metastable to the ground state only occurs in a magnetic dipole transition (singlet–triplet intercombination). Because of that the A-band has a low transition probability and its upper energy level has a relatively long life time (approx. 7 s). The big advantage of the $b^1\Sigma_g^+$ is its energy (1.63 eV) which is within the average energy range of electrons in most electrical discharges (low-pressure or atmospheric).[10]

Water vapor is present in many atmospheric plasma discharges in ambient air. Thus, oxygen as a part of a molecule could also be recorded over H_2O and/or the OH spectral emissions. In this work, only the OH emission is recorded. The OH radical with Q_1 band-head at $\lambda = 308.986$ nm (OH309) and transition $A^2\Sigma^+$ $(v = 0)$–$X^2\Pi$ $(v' = 0)$ has been recorded in all experimental conditions. The OH309 emission can be used for a thermal analysis of the plasma. The rotational temperature was measured from intensities of components of the Q_1 branch of the (0, 0) band for the electronic transition OH radical as it is close to the gas temperature.[11,12] The upper energy level of OH309 is metasable with an energy of 4.17 eV. The ionization energy of the OH molecule (13.18 eV) is just slightly lower than the ionization energy of a neutral hydrogen (13.62 eV) and both species (OH and H) are produced through H_2O dissociation.

2.3 *Hydrogen and nitrogen spectral emissions*

Atomic hydrogen (H I) is studied using the emission of the Balmier-α line ($\lambda = 656.279$ nm; $n = 2$–3). The upper energy level of the Balmier-α line has an energy of 12.09 eV. The lower energy level (10.20 eV) of the Balmier-α line is a resonant energy level in atomic Hydrogen. This resonate level has the highest transition probability, i.e., the shortest lifetime, in a hydrogen atom. Thus, quenching of the $n = 2$ atomic hydrogen energy level is most unlikely. A spectral intensity of the Balmier-α line could therefore be used for the density estimation of atomic hydrogen.

Nitrogen spectra are almost always found to be present in open air electrical discharges. In this research, one of the goals is to minimise the nitrogen spectral emission by optimizing the experiment. The only recorded nitrogen emission, in this work, is the second positive system with the band-head at $\lambda = 337.14$ nm and transition $C^3\Pi_u$ $(v = 0)$–$B^3\Pi_g$ $(v' = 0)$. This molecular nitrogen emission (N_2337) is of frequent occurrence as an impurity in the spectra of atmospheric plasma discharge. The upper and lower energy levels of N_2337 spectral emission have energies of 11.03 and 7.35 eV, respectively. The ionization energy of N_2 molecule is 15.58 eV.

2.4 *The setup*

This OES study was carried out on the plasma jet formed using the SurFx Atomflo™ 400L atmospheric plasma system. This type of plasma source is widely used for the plasma treatment of polymers in order to enhance surface energy.[12] The source operates at a rf frequency of 27.12 MHz and forms a plasma 5 cm wide, using its AH-500L beam applicator (Fig. 1). The RF power is shown on the controller of plasma source. The controller includes an RF generator with a fast auto-tuning matching network.[13]

Since it is very difficult to directly measure the output power of the SurFx plasma source, due to its closed box design, it is useful to calculate the thermal energy transfer of the plasma. Thermal imaging of a ceramic substrate, mounted below the jet, was obtained using an InfraTec Vari CAM high-resolution infrared thermographic camera and a K-type thermocouple. The measurement procedure builds on previous work, reported in literature.[12,14] An alumina ceramic (*W*) 21 cm, (*L*) 27 cm, and (*H*) 0.4 cm was chosen as the substrate, as it has a high specific heat capacity (850 $J \cdot g^{-1} \cdot K^{-1}$).[14] Using thermal imaging data, the thermal power transfer (P) can be estimated by measuring the surface temperature rise and the associated affected surface area. The data is then used to determine the time-dependent heating process using[15]

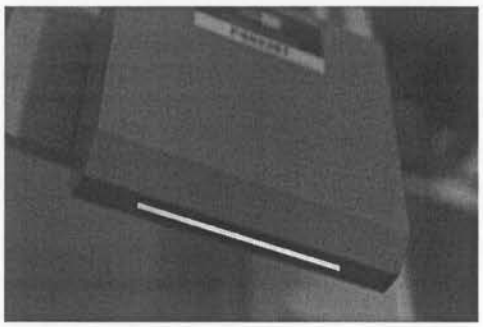

Fig. 1. (Color online) Photograph of SurFx Atomflo™ plasma source with 5 cm long applicator orifice.

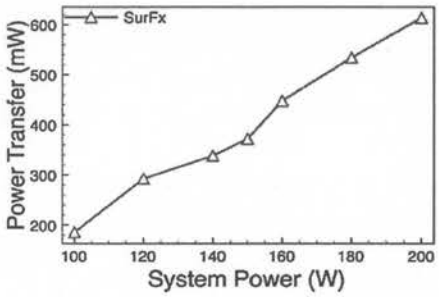

Fig. 2. Calculated thermal energy transfer values from the SurFx source to a ceramic substrate, placed 16 mm below the plasma nozzle, at the indicated processing powers.

$$P = m \cdot C_P \cdot \frac{\Delta T}{\Delta t}. \quad (1)$$

In Eq. (1), m represents the mass of the heated region, C_P is specific heat capacity of the substrate ($J \cdot g^{-1} \cdot K^{-1}$), while $\Delta T/\Delta t$ is the change in substrate temperature (T, in K) in relation to the time (t, in s). Thermal data was obtained while the plasma applicator head was mounted 16 mm above the ceramic surface. After ignition of the plasma, the change in temperature of the ceramic's surface was recorded until a steady state maximum temperature was reached. This was repeated for input process powers in the range of 100–200 W (as indicated in Fig. 2). Using the IRBIS 3 plus software package, supplied with the thermal imaging camera, the average temperature was calculated for a 1×1 cm^2 section of the ceramic substrate, positioned directly under the plasma jet, 15 and 30 s after the plasma was ignited. It should be noted that some thermal energy will be lost to the surrounding ambient in the 16 mm between the plasma nozzle and the ceramic substrate and so the calculations presented in this section do not represent the absolute energies of the plasmas investigated. The differences in the ceramic's temperature values (at 15 and 30 s) were used as the ΔT values in Eq. (1). The total mass of the 21×27 cm^2 ceramic substrate was measured to be 915 g; the mass of the 1 cm^2 ceramic area treated was therefore calculated to be

1.6 g. Since the same time interval, of 15 s, is used as the Δt function for all of the calculations, the thermal power transfer is directly proportional to the change in temperature of the substrate. The thermal power transfer to the ceramic plate is therefore calculated to be

$$P = 91.45 \cdot \Delta T. \quad (2)$$

Figure 2 shows the thermal energy transfer from the plasmas formed using the SurFx plasma jet system. A relatively linear relationship between system input power and thermal energy transfer is observed. Thermal energy transfer was in the range of 185–615 mW, at the conditions investigated.

The SurFx unit can generate plasma using He–O_2 gas mixtures (in the range of 100–200 W). The input variables for this system are strictly limited by the equipment manufacturer, i.e., helium gas needs to flow at a constant flow rate of 30 l/min, while oxygen gas input varies with plasma power. The oxygen flow rate was maintained at less than 3% of the helium flow rate at all times. Oxygen, which forms strong oxidising agents once injected into a helium plasma, is used as the source of reactive species in this study. More details about the experimental setup is presented in.[12,16,17] A feature of this source is the relatively contained plasma, which is confined almost entirely inside the applicator housing. This combined with the relatively high He flow rate maintains a relatively un-contaminated plasma, despite its direct exposure to the atmosphere.

Optical emission spectroscopy was carried out using a low resolution USB4000 spectrometer. The OES technique is based on the integration of measured signals over a line of sight observation. Despite this limitation however, OES is a non-intrusive diagnostic technique, which is commonly used to detect light emitted by excited species from plasma discharges. Experiments were carried out to investigate species intensity with varying power and time.[12] This resulted in a matrix of 64 experiments. OES data is recorded at the central point along the beam applicator, at 0, 15, 30, 45, 60, and 75 s after the plasma was struck (i.e., the duration of a processing time), for all plasma powers. These OES experiments were repeated at two other points along the beam applicator's orifice, as outlined in Ref. 12. A typical He–O_2 absolute intensity spectrum, recorded at 200 W after 30 s, is shown in Fig. 3. The helium–oxygen gas velocity during this experiment was calculated to be 6.9 m/s and has a laminar flow with a Reynolds number around $Re = 158$.[18] This figure also shows a helium spectrum recorded at a more typical gas flow of 10 l/min (dashed line). The gas velocity during this experiment was found to be 0.8 m/s and flow was found to be laminar with $Re = 106$.[18] It was established that 13 different atomic and molecular spectral emission existed in the plasma. In order to truly establish species importance at the various processing parameters, it was necessary to integrate the area under the emission peaks[8] for each OES spectra and to calculate a quantum efficiency of the spectral system (the spectrameter, fiber optic cable, lens, etc.).

The area under the emission peaks shown on Fig. 3, were measured and expressed in units of mW/cm^2 for a 1 s of integration time. The low resolution of the spectrometer has no influence on the profiles separation and the recorded continuum emission is very low. There are small continuum

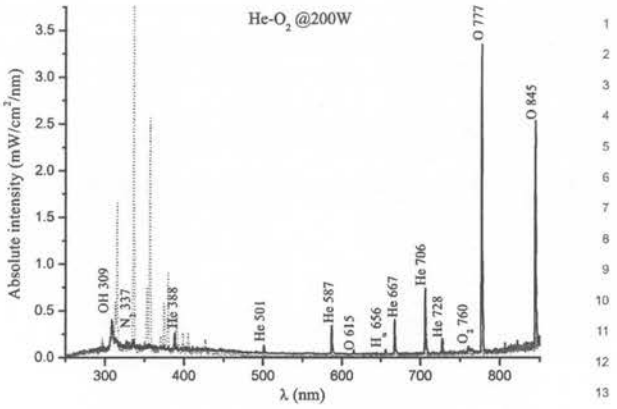

Fig. 3. (Color online) Spectrum of He–O_2 plasma discharge (solid line) recorded 30 s after the plasma was struck. The importance of OH309, $N_2$337, He388, etc. is discussed in Sects. 2.1–2.3. Also included is a typical helium plasma spectrum observed in an open air discharge (dashed line).[18]

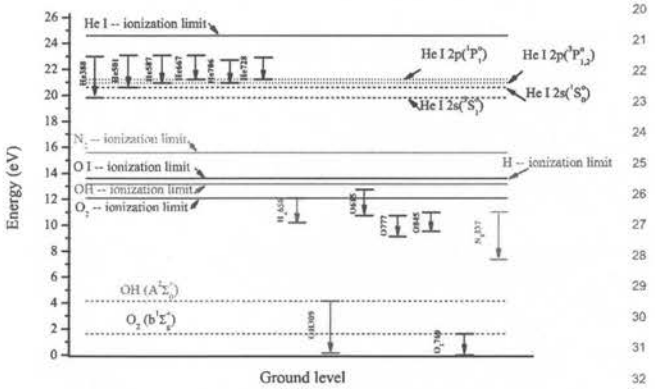

Fig. 4. (Color online) Energy diagram of the spectral emission from Fig. 3. All spectral line labels are the same as on Fig. 3.

emissions between 300 and 400 nm, as well as at wavelengths higher than 800 nm. The low continuum emission indicates that gas temperature is not high, i.e., it is not drastically different from the ambient temperature.

3. Results and Discussion

As well as optical spectra (Fig. 3), (nonradiative) energy transfer among different plasma species is also important for plasma diagnostics. The energy diagram in Fig. 4 takes into account the energy levels of all spectral profiles from Fig. 3.

Figure 4 shows clear separation among helium energy levels and the energy levels of other emitters in the plasma. Helium has the highest excited energy states and metastable levels and this needs to be taken into consideration when other species are being created in the plasma.

The He emission at 706 nm, with a threshold energy of 22.7 eV and a radiative decay lifetime of the upper state of 35 ns,[5] is an indicator of energetic electrons.[19] The He706 is produced by radiative dissociation of the He_2^* dimer, which is formed by a recombination process from the metasable He atom. Even small amounts of nitrogen drastically change the metasable helium density by fast Penning ionization with N_2.[19] Thus the intensity of the He706 decreases if the content of air in the discharge is too high. Figure 5 shows the He706

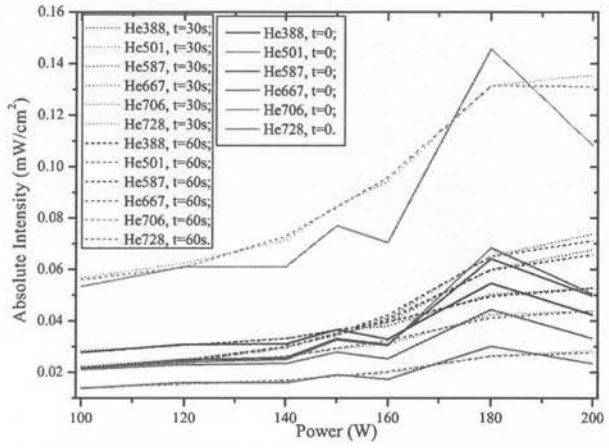

Fig. 5. (Color online) Absolute intensity of helium atomic spectral liens at three different time intervals from the striking of the discharge: solid line, $t = 0$ s; doted line, $t = 30$ s; dashed line, $t = 60$ s. All labels are the same as Fig. 3.

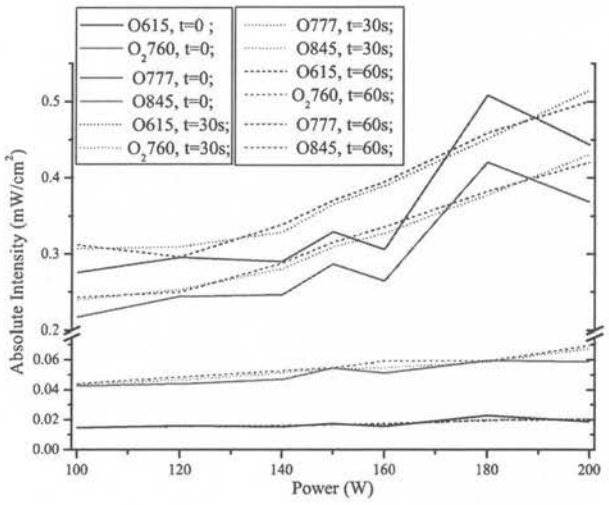

Fig. 6. (Color online) Absolute intensity of oxygen's atomic and molecular spectral emissions at three different time intervals from the striking of the discharge: solid line, $t = 0$ s; doted line, $t = 30$ s; dashed line, $t = 60$ s. All labels are the same as Fig. 3.

emission, as well as other helium spectral emissions, all of these were observed to increase with processing time and applied rf power. Figures 6 and 7 show the oxygen and nitrogen spectral emissions, respectively. The O777 and O845 show (Fig. 6) similar trends to the He706 (Fig. 5) with respect to processing time and applied rf power. The other two oxygen spectral emissions (O615 and O_2706) do not Display significant intensity fluctuations with changes in processing time or applied rf power. The mechanisms of creation the O615 and the O_2706 are discussed in Sects. 2.2 and 2.3, and it will be more discussed in this section in conjunctions with the He706 spectral emissions. The absolute spectral emission of molecular nitrogen (Fig. 7) shows oscillation around an average value for each of the three different time intervals. These oscillations are suppressed with the processing time.

Figure 5 shows that the high helium flow rate overrules nitrogen's importance in a plasma discharge. The nitrogen

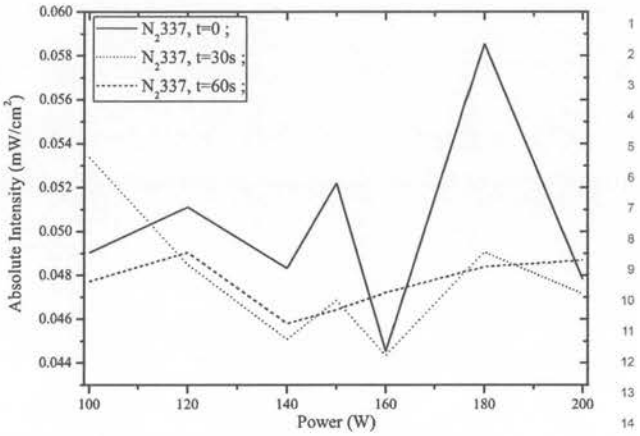

Fig. 7. Absolute spectral intensity of nitrogen molecular band at 337 nm and at three different time intervals from the striking of the discharge: solid line, $t = 0$ s; doted line, $t = 30$ s; dashed line, $t = 60$ s. All labels are the same as Fig. 3.

spectral emission is present only through N_2337 (see Fig. 3), which is a unique case since the majority of open air plasma discharges are very rich in nitrogen emission.[20] The N_2337 nm emission lines correspond to the following transition $N_2(C^3\Pi_u{}^+) \rightarrow N_2(B^3\Pi_g{}^+)$.[21] The $N_2(C^3\Pi_u{}^+)$ state can be populated in several ways and has a lifetime of 38 ns. Firstly, it can be populated through the direct electron impact excitation from the N_2 ground state: $N_2(X^1\Sigma_g{}^+)_{v=0} + e_{fast} \rightarrow N_2(C^3\Pi_u{}^+)_{v'=0,1} + e_{slow}$, where the threshold energy of fast electrons equals to 11.5 eV. In this case, the population rate for the upper level of the N_2337 transition is proportional to the N_2 ground state number density and the density of fast electrons. A second possible population mechanism of the $N_2(C^3\Pi_u{}^+)$ state is through the electron recombination of $N_2{}^+(X^2\Sigma_g{}^+)$ followed by decay. The second mechanism is less probable as there is no significant spectral emission recorded for a wavelength of 391–393 nm (Fig. 3). In this spectral region, nitrogen should has very strong emissions, which are created by the electron transition from $N_2{}^+$ $(B^2\Sigma_u{}^+,\ v = 0)$ to $N_2{}^+$ $(X^2\Sigma_u{}^+,\ v' = 0)$ state. The $N_2{}^+$ $(B^2\Sigma_u{}^+)$ is populated through the Penning reaction and/or the charge transfer from $He_2{}^+$ ions. The temporal profile of the 391–393 nm line therefore reflects the evolution of the helium metastables and molecular ions.[22] Similarly, the helium line at 706 nm indicates the presence of either energetic electrons or $He_2{}^+$ ions and high energy electrons.[22] The absence of a strong/any $N_2{}^+$ emission supports the suggestion that there was an insufficient number of helium metastable atoms. The lifetime of electrons at matastable levels should be in the order of μs or longer[5] but, due to its high quenching rates, it is drastically lower.[23] These results are similar to those previously reported in Ref. 7, where it was shown that helium metasable atoms were shown to be less important in influencing plasma chemistry as gas flow rates increased. As it is presented in Fig. 5, two helium spectra emissions (He388 and He501), which represent helium metastable atoms, have the lowest intensity within triplet/singlet helium states. The other four helium lines exhibit much higher intensities and these lines represent the helium atom in its ground state (as discussed earlier). The temporal profiles of all helium spectral lines are similar

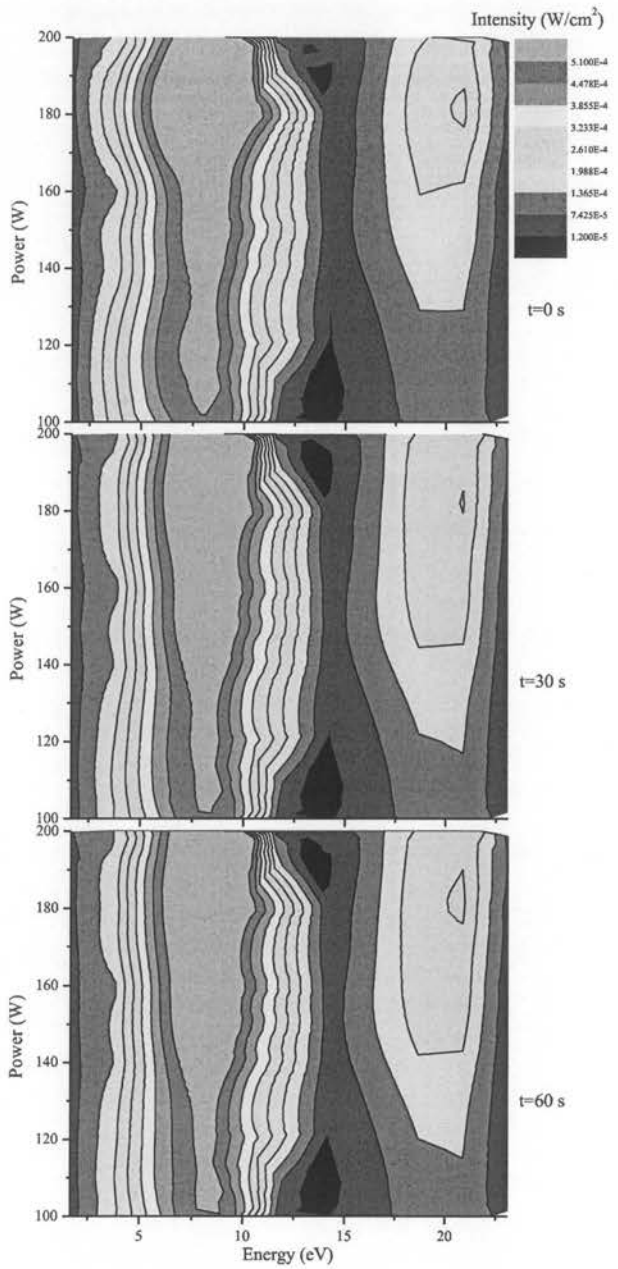

Fig. 8. (Color online) The total spectral intensity for all 13 spectral profiles at three different times (0, 30, and 60 s) from the ignition of the discharge.

(Fig. 5), and this is a case for all other emissions detailed in Fig. 3. Figure 8 shows the absolute spectral intensities as a function of the rf power, processing time and the energy of the upper energy levels.

The spectra's intensities shown in Fig. 8 stay almost constant up to 60 s time period investigated, which indicates a high degree of plasma stability, and this is clearly very important for any technological application. The difference in the intensities of the excited plasma species in Fig. 8 were probably related to their different life spans and the energy thresholds. The peak intensity, in Fig. 8 of 8 eV, gives an indication of the dynamics of energetic electrons. This suggests that the profiles of excited plasma species may be influenced by both their lifetimes and the dynamics of energetic electrons.

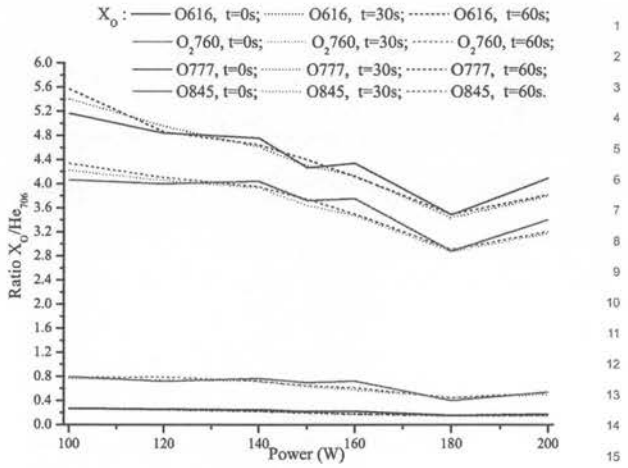

Fig. 9. (Color online) Temporal oxygen spectral emission: solid line, $t = 0$ s; doted line, $t = 30$ s; dashed line, $t = 60$ s.

The optical emission spectrum (Fig. 3) consists of, atomic and molecular oxygen, as well as helium, hydrogen and nitrogen species emissions. Oxygen could come from the ambient air, the He–O_2 gas mixture or from H_2O dissociation. Electron impact excitation of molecular oxygen, at low collision energies, is of particular importance because of its role in atmospheric physics. Transitions between the $X^3\Sigma$ ground state and the two lowest $a^1\Delta$, and $b^1\Sigma$ electronically excited states are forbidden by optical dipole selection rules. However the transitions occur as a result of higher-order interactions. The metastable $b^1\Sigma$, state is important because of its long lifetime of 7 s.[24] It also permits the production of sufficient numbers of atomic oxygen to enable the study of excited molecular species by means of collision scattering experiments. The very long lifetime of the molecular oxygen metastable molecule makes its quenching very efficient. The quenching of singlet molecular oxygen involves the deactivation of the excited state of the molecule.[10] Deactivation can be accomplished by either physical or chemical quenching. Physical quenching only results in the deactivation of singlet oxygen to its ground state, with no oxygen consumption or product formation. In contrast chemical quenching results in singlet oxygen reactions with quencher R to produce RO_2. The two major mechanisms of $^1O_2$ quenching are known to be energy transfer and charge transfer quenching.

Energy transfer quenching is the reverse reaction through which singlet oxygen is formed.[25] It involves formation of triplet quencher and ground state oxygen ($^1O_2 + Q \rightarrow {}^3O_2 + Q$).

Charge transfer quenching involves the interaction between the electron-deficient $^1O_2$ molecule and electron donors to form a charge transfer complex.[25] Intersystem crossing restrictions are relaxed in the complex,[10] which can then dissociate into donor and ground state oxygen. The spectral radiation based on this mechanism includes: O_2760, O615, O777, and O845 emissions. Figure 9 presents the atomic and molecular oxygen emission in the respect to the He706 emission. It can be observed that the temporal emission profile of the O777 and O845 in this figure is different to that of nitrogen and helium. The weak temporal dependence of the O777 and O845 emission pattern suggests

that $O(^5P)$ and $O(^3P)$ are mainly populated by the direct excitation of atoms by electron impact, with a lifetime of upper energy levels of 29 and 32 ns respectively. Underpinning that He706 emissions, detected in helium discharges with a small concentration of impurities, can be used to indicate the presence of energetic electrons. The O777 and O845 cannot be created by a dissociative recombination with the ground state O_2^+ because the rate is strongly peaked toward low energy electrons[26] and there is insufficient energy for these to produce the excited atoms of interest since the difference between the ionization potential of O_2 (12.07 eV) and the bond dissociative energy (5.09 eV)[27] is substantially less than the atomic excitation energy (11 eV) for the $O(^5P)$ and $O(^3P)$ states. Another option for the creation of O777 and O845 is the dissociative excitation of the molecular oxygen. The emission of O_2760 is almost constant with time and with the rf power, and it does not follow the trends of the O777 and O845 emissions (see Fig. 6). The slopes of the O777 and O845 are an order of magnitude greater than the O_2760 slope. The similar trends of these emissions are also recorded in Fig. 9. It is concluded from this study that the general interpretation that a dissociative molecule oxygen excitation is the dominant mechanism for an O777 emission, and the atomic oxygen excitation is much more important for an O845 emission,[28] was found not to be the case for a high helium flow rate plasma source. Another possible channel for creation of O777 and O845 could also be radiative cascading from the higher, exited levels in an oxygen atom.[8] The O615 spectral line has an upper energy level lifetime of 43 ns, while its lower energy level is the same as the upper energy level of O777. The intensity of O615 is insensitive to the change of rf power or the processing time (Fig. 6). This similar dependence could be seen in Fig. 9 for this emission. This indicates that the direct excitation of an oxygen atom to a high laying energy level (4d $^5D^o$) by high energetic electrons, is not important for creating this (O615) emission. Thus the only mechanism important for the creation of oxygen radicals in the states 3p ^5P and p ^5P, in a high flow helium atmospheric plasma discharge, is a direct excitation of atoms by high energetic electrons (the He706 emission pattern). In Fig. 9 the minimum ratio, recorded at 180 W, could be attributed to a change (increase or decrease) in T_e (i.e., EEDF) or to a change in helium metastable kinetics. Namely, the X_O/He706 increase suggests that the electron energy distribution shifted towards a higher energy value. Electron energy distribution changes affect the dissociation coefficient of the oxygen molecule.[29] Thus, this electron energy distribution change, induced by the addition of oxygen flow to the fixed helium flow, introduced the change in atomic oxygen in the plasma.

The OH band ($A^2\Sigma^+$, $v = 0$–$X^2\Pi$, $v' = 0$) was investigated and shows a red degradation with main band head at 308.986 nm.[9] The OH radicals could be produced through H_2O dissociation or/and is produced in the isothermal flow plasma jet by the reaction $H + NO_2 \rightarrow NO + OH$, where the H atoms are formed by the plasma discharge of highly humid ambient air and helium mixtures. The second channel is mostly unlikely since the high helium flow rate limits the importance of nitrogen. Since the dissociation of molecules (H_2O) is most likely described by the gas kinetic temperature,

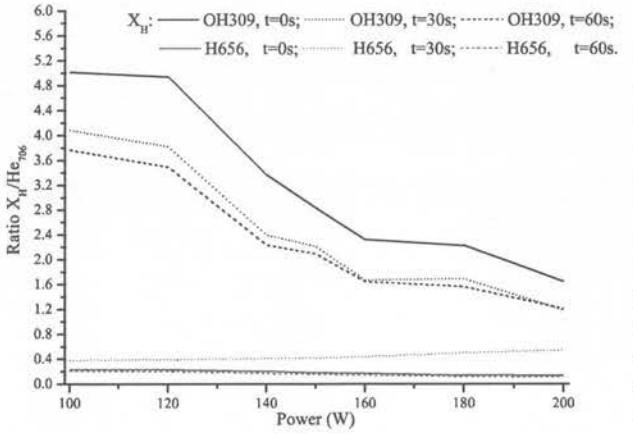

Fig. 10. (Color online) Temporal OH309 and H656 spectral emissions: a solid line, $t = 0$ s; a doted line, $t = 30$ s; a dashed line, $t = 60$ s.

the radical OH can be used as an indication of temperature in an ambient gas plasma discharge.[30] The OH309 emission described in this work is used for gas temperature measurement and was benchmarked against infrared thermal imaging[12] and the gas temperature was in the range 40–70 °C. Overall the OH band ($A^2\Sigma^+$, $v = 0$–$X^2\Pi$, $v' = 0$) was observed to be very sensitive/accurate for a plasma gas temperature in the range of 300–6000 K. Quantification of OH radicals in atmospheric pressure plasma jets can be useful for the understanding of OH formation mechanisms and plasma generation. OH radicals exist at a relatively large distance from a main plasma plume of atmospheric pressure helium plasma jets.[11] Figure 10 shows the ratio of both the OH and H spectral intensities to He706.

With increases of rf power, as well with processing time, the intensities of OH309 (not shown) has a ±50% fluctuation around mean value of 0.25 mW/cm^2, during the same time the H656 (not shown) spectral intensity monotonously increases four times. By dividing these intensities by the He706 emission intensity (which represents high energy electrons) the graph in Fig. 10 was generated. This shows a monotonic decrease in the ratio of the intensities of OH309 (no intensity fluctuation) and a very small increase in the H656 signal. The energy required for a H_2O dissociation is 5.03 eV and the product of this dissociation is an OH molecule and a hydrogen atom. Figure 10 suggests that the electron energy distribution function is shifted towards a higher energy.

4. Conclusion

Open air plasma discharges are widely used for surface activation and cleaning. The reactive species created in these discharges could have a significant impact on technology processes and on the environment. Electrical discharges in ambient air produce some very (potentially) hazardous species such as: NO_x, OH^*, H^*, O^*, O_3, and/or H_2O_2. From this study it was concluded that helium atmospheric plasma jets, with a high gas flow rates, are more stable (no arcing) and they do not depend on impurities (N_2, O_2, ...) to sustain the plasma discharge. Nitrogen contamination increases the gas temperature due to its lower heat conductivity than that of a helium atom. In an optimized helium gas flow, a plasma

discharge has no turbulent flow, i.e., the plasma jet is stable and quiet. The large applicator head allows a laminar flow of gas which is well structured, with a hot and bright core. Moreover, the small amount of O_2 added to the plasma forming gas (helium) causes the plasma length to be reduced to couple of millimeters.

In the vast majority of helium discharges in ambient air, emission spectra clearly show the efficiency of helium to excite the impurities absorbed on electrodes, or existing as traces within an atmosphere. In this work, with a high helium gas flow rate, the significance of spectral emissions other than the helium atom is observed to be unimportant. Wavelength resolved optical emission profiles suggest that, the helium emission indicates that high energy electrons (spectral emission at 706 nm) are more important than helium metastables (spectral emissions at 388 and 501 nm), on the overall spectral emission. The lifetime of helium metastables energy levels are indicated to be drastically reduced as a result of quenching.

The high helium gas flow rate narrows the production channel of the oxygen radicals to the direct electron impact (excitation process) from the ground state of the O I. The general interpretation that the dissociative molecule oxygen excitation is the dominant mechanism for O777 emission, and that atomic oxygen excitation is much more important for O845 emission was found not to be the case for the high He–O_2 flow rate plasma discharge.

Overall the high helium flow rate is used in an attempt to minimize the ratio of gas convection to chemical reaction time scale (recombination). This favors the rapid transport of newly created radicals and excited species to the surface under treatment. The addition of a low levels (<3%) of an electronegative gas (oxygen) to helium gas causes a reduction of the electron density and consequently, a reduction of the electrical conductivity. This also causes an increase in the sustaining voltage and consequently, in the electric field strength. Therefore the mean electron kinetic energy is increased, and this leads to an increase of the excitation temperature.

Acknowledgments

This material is based upon works supported by the Science Foundation Ireland under Grant No. 08/SRC/I1411 as well as the "Fresh-Pack" project funded by the National Development Plan, through the Food Institutional Research Measure, administered by the Department of Agriculture, Food and the Marine, Ireland. V. Milosavljević is also grateful to the Ministry of Education and Science of the Republic of Serbia under Grant No. OI171006.

*vm@dit.ie

1) Y. Ohguchi and K. Takahama, J. Phys. Soc. Jpn. **55**, 3889 (1986).
2) S. Yamada, H. Yoshimura, and M. Tachibana, J. Phys. Soc. Jpn. **79**, 054708 (2010).
3) C. Yubero, M. D. Calzada, and M. C. Garcia, J. Phys. Soc. Jpn. **74**, 2249 (2005).
4) R. Brandenburg, J. Ehlbeck, M. Stieber, T. v. Woedtke, J. Zeymer, O. Schlüter, and K.-D. Weltmann, Contrib. Plasma Phys. **47**, 72 (2007).
5) Yu. Ralchenko, A. E. Kramida, J. Reader, and NIST ASD Team, NIST Atomic Spectra Database (ver. 4.1.0) (National Institute of Standards and Technology, Gaithersburg, MD, 2013) [http://physics.nist.gov/asd].
6) V. Milosavljević, D. Popović, and A. R. Ellingboe, J. Phys. Soc. Jpn. **78**, 084501 (2009).
7) K. Tachibana, Y. Kishimoto, and O. Sakai, J. Appl. Phys. **97**, 123301 (2005).
8) V. Milosavljević, A. R. Ellingboe, and S. Daniels, Eur. Phys. J. D **64**, 437 (2011).
9) G. F. R. S. Herzberg, *Molecular Spectra and Molecular Structure I. Spectra of Diatomic Molecules* (D. van Nostrand, Princeton, NJ, 1950) 2nd ed.
10) S. Popović, M. Nikolić, J. Upardhyay, and L. Vučković, AIAA 2010-5042 (2010).
11) S. Pellerin, J. M. Cormier, F. Richard, K. Musiol, and J. Chapelle, J. Phys. D **29**, 726 (1996).
12) M. Donegan, V. Milosavljević, and D. P. Dowling, Plasma Chem. Plasma Process. **33**, 941 (2013).
13) S. E. Babayan and R. F. Hicks, US Patent 7329608 (2008).
14) D. P. Dowling, F. T. O'Neill, S. J. Langlais, and V. J. Law, Plasma Processes Polym. **8**, 718 (2011).
15) K.-D. Weltmann, E. Kindel, R. Brandenburg, C. Meyer, R. Bussiahn, C. Wilke, and T. von Woedtke, Contrib. Plasma Phys. **49**, 631 (2009).
16) R. J. Zaldivar, J. Nokes, G. L. Steckel, H. I. Kim, and B. A. Morgan, J. Compos. Mater. **44**, 137 (2010).
17) R. J. Zaldivar, J. Salfity, G. Steckel, B. Morgan, D. Patel, J. P. Nokes, and H. I. Kim, J. Compos. Mater. **46**, 1925 (2012).
18) C. E. Nwankire, V. J. Law, A. Nindrayog, B. Twomey, K. Niemi, V. Milosavljević, W. G. Graham, and D. P. Dowling, Plasma Chem. Plasma Process. **30**, 537 (2010).
19) N. K. Bibinov, A. A. Fateev, and K. Wiesemann, J. Phys. D **34**, 1819 (2001).
20) J. L. Walsh, J. J. Shi, and M. G. Kong, Appl. Phys. Lett. **89**, 161505 (2006).
21) A. Qayyum, S. Zeb, M. A. Naveed, S. A. Ghauri, M. Zakaullah, and A. Waheed, J. Appl. Phys. **98**, 103303 (2005).
22) G. Nersisyan and W. G. Graham, Plasma Sources Sci. Technol. **13**, 582 (2004).
23) S. Suzuki, H. Itoh, H. Sekizawa, and N. Ikuta, J. Phys. Soc. Jpn. **62**, 2692 (1993).
24) T. G. Slanger and R. A. Copeland, Chem. Rev. **103**, 4731 (2003).
25) B. Halliwell and M. C. John, *Free Radical in Biology and Medicine* (Clarendon, Oxford, U.K., 1982) 2nd ed.
26) M. A. Biondi, in *Principles of Laser Plasmas*, ed. G. Bekefi (Wiley, New York, 1976) Chap. 4.
27) K. P. Huber and G. Herzberg, *Constants of Diatomic Molecules* (Van Nostrand Reinhold, New York, 1979).
28) R. E. Walkup, K. L. Saenger, and G. S. Selwyn, J. Chem. Phys. **84**, 2668 (1986).
29) H. S. W. Massey, *Electronic and Ionic Impact Phenomena* (Clarendon, Oxford, U.K., 1969) Vol. II.
30) S. Tsurubuchi, T. Iwai, and T. Horie, J. Phys. Soc. Jpn. **36**, 537 (1974).